Dalton Transactions

PAPER

View Article Online
View Journal

Cite this: DOI: 10.1039/c9dt00334g

$Ru(O_2CCF_3)_2(PPh_3)_2$ and ruthenium phosphine complexes bearing fluoroacetate ligands: synthesis, characterization and catalytic activity†

Daniela A. Hey,‡[a] Pauline J. Fischer,‡[a] Walter Baratta *[b] and Fritz E. Kühn *[a]

Received 24th January 2019,
Accepted 7th March 2019

DOI: 10.1039/c9dt00334g

rsc.li/dalton

The dinuclear ruthenium(II) phosphine complexes $Ru_2Cl(O_2CCH_xF_{3-x})_3(PPh_3)_4(\mu\text{-}H_2O)$ (x = 0, 1, 2), containing fluoroacetate ligands, were prepared from $RuCl_2(PPh_3)_3$ and $NaO_2CCH_xF_{3-x}$ in ^{t}BuOH. The X-ray characterization of these complexes reveals a bridging water molecule, stabilized by hydrogen bonds with the fluoroacetate ligands. The isolation of the complex $Ru(O_2CCF_3)_2(PPh_3)_2$ is described, starting from $RuCl_2(PPh_3)_3$ or $Ru_2Cl(O_2CCF_3)_3(PPh_3)_4(\mu\text{-}H_2O)$ and TlO_2CCF_3, correcting the reported preparation in which $Ru_2Cl(O_2CCF_3)_3(PPh_3)_4(\mu\text{-}H_2O)$ was obtained. $Ru(O_2CCF_3)_2(PPh_3)_2$ easily reacts with CO, affording $Ru(O_2CCF_3)_2(CO)_2(PPh_3)_2$. The protonation of $Ru(OAc)_2$(dppb) with trifluoroacetic acid in the presence of bidentate O and N donor ligands affords the complexes $Ru(O_2CCF_3)_2$(dppb)(LL) (LL = ethyleneglycol, ethylenediamine), which are catalytically active in the transfer hydrogenation of ketones with 2-propanol. In the reduction of cyclohexanone, the glycol derivative displays a higher catalytic activity than the diamine complex, reaching a TOF of 22 000 h^{-1}.

Introduction

Ruthenium(II) phosphine carboxylate complexes have been investigated in detail for the catalytic hydrogenation of olefins and carbonyl compounds in the last few decades.[6–12] Since the 1970s, ruthenium complexes containing trifluoroacetate ligands are known as active catalysts for the dehydrogenation of alcohols and the hydroformylation of alkenes.[13–15] The electron-withdrawing nature of trifluoroacetate in comparison with acetate and the resulting lability of the perfluorinated ligand set a detailed investigation of the reactivity of ruthenium(II) trifluoroacetato phosphine derivatives in motion.[17–23] Most literature-known trifluoroacetate complexes contain ancillary ligands, such as carbonyl, hydride or carbene, while only a few examples of the general formula $Ru(O_2CCF_3)_2P_2$ (P = PPh_3, PCy_3) can be found in literature.[16,24] In the 1990s, similar structures emerged, as chiral diphosphines were explored in combination with the trifluoroacetate ligand, affording active catalysts for enantioselective hydrogenation reactions (Fig. 1).[1–5] The isolation of these complexes proved to be difficult in some cases.[2] The active species were therefore often generated *in situ*, for instance from ruthenium cyclooctadiene precursors, or the formed complexes were described as solvato- or water-adducts.[4,5,25,26]

The difficult isolation of well-defined derivatives most probably led to ruthenium(II) diphosphine bis(trifluoroacetato) complexes being scarcely examined nowadays, even though they offer promising catalyst precursors on account of their facile ligand dissociation.[25,27] Based on this property, together with the enhanced performance of several catalysts by the addition of trifluoroacetic acid (TFA) to the reaction mixture,[28–30] it was intended to synthesize trifluoroacetate complexes of the general formula $Ru(O_2CCF_3)_2P_2$ (P = mono- or bidentate phosphine ligand) and to employ them in the catalytic hydrogenation of ketones.

The synthesis of $Ru(O_2CCF_3)_2(PPh_3)_2$ (**1**) has previously been described by Sanchez-Delgado and Wilkinson[14] by reaction of $RuCl_2(PPh_3)_3$ with TFA and $NaHCO_3$ in boiling ^{t}BuOH (Scheme 1, **I**), following the procedure reported for the preparation of $Ru(O_2CCH_3)_2(PPh_3)_2$.

[a]*Molecular Catalysis, Catalysis Research Center and Department of Chemistry, Technische Universität München, Lichtenbergstr. 4, 85747 Garching bei München, Germany. E-mail: fritz.kuehn@ch.tum.de*

[b]*Dipartimento di Scienze AgroAlimentari, Ambientali e Animali (DI4A), Università di Udine, Via Cotonificio 108, I-33100 Udine, Italy*

†Electronic supplementary information (ESI) available: Crystallographic details, NMR data, and catalytic kinetics. CCDC 1892668–1892675. For ESI and crystallographic data in CIF or other electronic format see DOI: 10.1039/c9dt00334g

‡These authors contributed equally to this work.

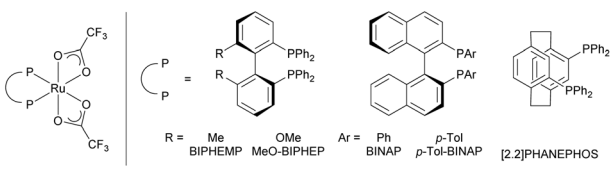

Fig. 1 Chiral $Ru(O_2CCF_3)_2P_2$ complexes employed as catalysts in enantioselective hydrogenation reactions.[1–5]

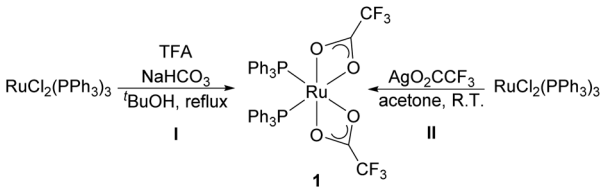

Scheme 1 Reported synthetic routes to obtain $Ru(O_2CCF_3)_2(PPh_3)_2$ (**1**) from $RuCl_2(PPh_3)_3$.[14,16]

Furthermore, a different procedure for the synthesis of **1** was reported by Yamamoto *et al.*, by reacting $RuCl_2(PPh_3)_3$ and AgO_2CCF_3 in acetone (Scheme 1, **II**).[16] However, **1** has been poorly characterized only by IR spectroscopy and elemental analysis.[14] Other pathways to obtain $Ru(O_2CCF_3)_2P_2$ complexes *via* Ru(η^3-methylallyl)$_2$(COD) have also been pursued, though only for phosphines different from PPh_3.[2,4,31]

Since the reproduction of the literature data proved to be difficult, these reactions were re-examined and a detailed study of the formation and characterization of fluoroacetate ruthenium phosphine complexes is described in this work. The reactivity of the ruthenium precursors and preliminary studies on their catalytic activity in the ketone transfer hydrogenation are reported as well.

Results and discussion

Synthesis of fluoroacetate ruthenium(II) complexes

Treatment of $RuCl_2(PPh_3)_3$ with trifluoroacetic acid (TFA, 5 equiv.) and $NaHCO_3$ (4 equiv.) in refluxing ^{t}BuOH[14] for 3 h affords the dinuclear complex **2** as an orange precipitate, which could be isolated in 85% yield (eqn (1)).

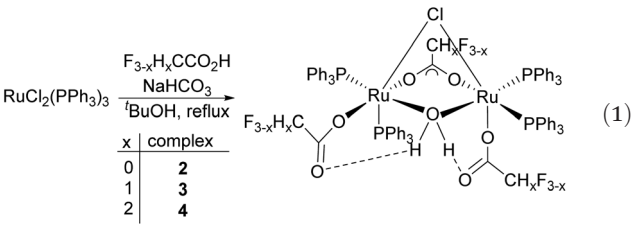

(1)

The X-ray crystal structure of **2** shows two ruthenium(II) centers in a pseudo-octahedral geometry, bridged by a chloride, a trifluoroacetate and a water molecule (Fig. 2). As expected, the Ru–O bond length of the bridging trifluoroacetate in *trans* position to PPh_3 is longer (Ru2–O2 = 2.1520(17) Å) than the Ru–O bond length in the *trans* position to the η^1-trifluoroacetate ligand (Ru1–O3 = 2.0947(17) Å) due to the strong *trans* influence of the phosphine ligand.[32–34] The Ru1–O1 and Ru2–O1 distances for the bridging water molecule are relatively long (Ru1–O1 = 2.2537(19) Å and Ru2–O1 = 2.2581(19) Å), indicating that H_2O is weakly coordinated. In addition, asymmetric O···H distances (1.754 Å and 1.888 Å) between the protons of the bridging water molecule and the oxygen atoms of the monodentate trifluoroacetate ligands indicate the presence of hydrogen bonds stabilizing the

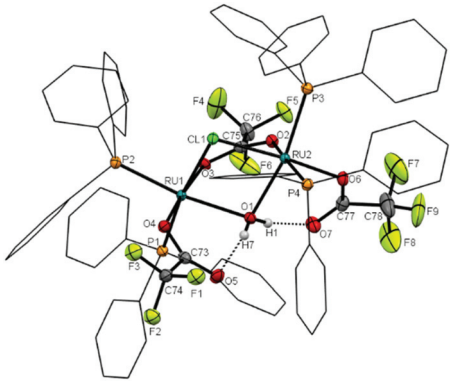

Fig. 2 ORTEP style drawing of the dinuclear complex **2**. Phenyl rings depicted in wireframe style. All hydrogen atoms but for H_2O omitted for clarity. Ru^{II} centers are bridged by TFA, Cl^- and H_2O. Hydrogen bond distances between O7···H1 and O5···H7 are found to be 1.754 and 1.888 Å, respectively.

complex.[35,36] Hydrogen bonding involving water and a tetrafluorosuccinate ligand has been reported for the related ruthenium(II) complex $[Ru(OCOC_2F_4OCO)(CO)(\mu\text{-}H_2O)(PPh_3)_2]_2$ by van Buijtenen *et al.*[37] Several water-bridged ruthenium(II) dinuclear species with a corresponding dinuclear Ru^{II}–H_2O–Ru^{II} structure can be found in the literature, namely $Ru_2Cl_4(\mu\text{-}H_2O)[P(3,5\text{-xylyl})_3]_4$, $Ru_2Cl_4(\mu\text{-}H_2O)(dppb)_2$, $[Ru(C_6H_9PCy_2)(CF_3COO)]_2(\mu\text{-}CF_3COO)_2(\mu\text{-}H_2O)$, $[Ru_2(C_2H_5)_2(CO)_4(\mu\text{-}H_2O)_4](CF_3SO_3)_2$ and $[\{\eta^5\text{:}\sigma\text{-}Me_2C(C_5H_4)(C_2B_{10}H_{10})\}Ru(\mu\text{-}H_2O)]_2$.[10,24,38,39]

In CD_2Cl_2, **2** exhibits two pairs of doublets in the ^{31}P NMR spectrum, at δ = 50.9 ppm (d, ^2J(PP) = 42.1 Hz), 50.3 ppm (d, ^2J(PP) = 42.1 Hz), 48.7 ppm (d, ^2J(PP) = 38.9 Hz) and 47.7 ppm (d, ^2J(PP) = 38.8 Hz), evidencing two asymmetrically bound triphenylphosphine ligands on each Ru center. The three singlets at δ = −74.52, −74.60 and −76.70 ppm in the ^{19}F NMR spectrum account for one monodentate trifluoroacetate moiety on each Ru center and a μ_2-trifluoroacetate bridging the two metal atoms. The ^{1}H NMR spectrum of **2** at room temperature shows the two protons of the bridging H_2O molecule as a broad singlet downfield shifted to δ = 9.51 ppm due to the presence of strong hydrogen bonds with the trifluoroacetate ligand. Upon cooling to −80 °C, the proton signal splits into two singlets at δ = 9.11 and 9.77 ppm, indicating that the two hydrogen atoms are chemically non-equivalent as a consequence of the hydrogen bonding to the TFA moieties (for NMR spectra see the ESI†). The NMR studies therefore indicate that complex **2** exhibits the same structure both in solution and in the solid state and that the stabilizing water molecule undergoes a rapid exchange of the two protons at room temperature, while this process can be inhibited at low temperatures on the NMR time scale.

The results contradict the formation of **1** from $RuCl_2(PPh_3)_3$ and TFA/$NaHCO_3$ in ^{t}BuOH as described by Sanchez-Delgado and Wilkinson.[14] The authors provide IR absorptions and elemental analysis data for the supposed complex **1**, which stand in complete agreement with those for the dinuclear species **2**. Note that the elemental analysis reported for **1** deviates significantly for F,[9,40] indicating that the authors had in fact isolated **2** but inter-

preted it as **1**. Furthermore, **1** has not been characterized by Yamamoto *et al.*, who reported the synthesis of **1** by the reaction of $RuCl_2(PPh_3)_3$ with AgO_2CCF_3.[16] Therefore, while the reaction of $RuCl_2(PPh_3)_3$ with CH_3CO_2Na leads to the corresponding mononuclear species $Ru(O_2CCH_3)_2(PPh_3)_2$, employment of CF_3CO_2Na affords the dinuclear complex $Ru_2Cl(O_2CCF_3)_3(PPh_3)_4(\mu\text{-}H_2O)$, containing chloride and water as bridging ligands, most likely due to the lower coordination ability of the trifluoroacetate with respect to the acetate anion.

To investigate the effect of the fluorine atoms on the coordination ability of the fluoroacetate ligands, $RuCl_2(PPh_3)_3$ was reacted with the salts $CF_{3-x}H_xCO_2Na$ (x = 1, 2). The reaction of $RuCl_2(PPh_3)_3$ with DFA and MFA (5 equiv.) and $NaHCO_3$ (4 equiv.) in boiling ^{t}BuOH (eqn (1)) for 3 h results in the formation of the dinuclear complexes **3** (42% yield) and **4** (51% yield) (Fig. 3 and 4).

The X-ray crystal structures of **3** and **4** are similar to that of **2**, showing two ruthenium(II) centers with pseudo-octahedral coordination geometry, bridged by chloride, water and the respective fluoroacetate. The formation of hydrogen bonds from the bridging water molecule to the η^1-fluoroacetate moieties likewise explains the formation of dinuclear complexes as most stable compounds under the applied conditions, analogous to the observations for the trifluoroacetate species **2**. Hydrogen bond lengths between the hydrogen atoms of the bridging water and the oxygen atoms of the terminal fluoroacetate ligands in **3** (1.735 Å and 1.887 Å) and **4** (1.705 Å and 1.888 Å) lie in the range of those found for **2** (Table 1). The slight decrease of the hydrogen bond lengths from **2** over **3** to **4** points towards a higher donor strength of the less fluorinated ligands, even though the difference is relatively small.

In solution, **3** and **4** exhibit two pairs of doublets in the ^{31}P NMR spectrum for four non-equivalent phosphine ligands, analogous to **2**. In the $^{19}F\{^1H\}$ NMR spectrum, the DFA ligands in **3** cause five singlets at δ = −124.08, −124.32, −124.33, −124.88 and −125.25 ppm, with the signal at δ = −124.88 ppm integrating for two F atoms, whereas the MFA ligands of **4** afford three singlets at δ = −216.38, −218.43 and −218.89 ppm for one η^1- and two η^2-MFA moieties. At room temperature, the bridging H_2O molecule causes signals at δ = 10.34 and 10.19 ppm in the ^{1}H NMR spectra of **3** and **4**, respectively. Upon cooling to −40 °C, the water signal of **4** splits into two singlets at δ = 10.27 and 11.54 ppm for the non-equivalent hydrogen-bonding protons, in accordance with **2**. Therefore, the NMR studies in solution are consistent with the measured solid-state crystal structures, indicating that **3** and **4** are formed as dinuclear species in contrast to $Ru(O_2CCH_3)_2(PPh_3)_2$. A summary of selected characteristics of **2**, **3** and **4** is given in Table 1.

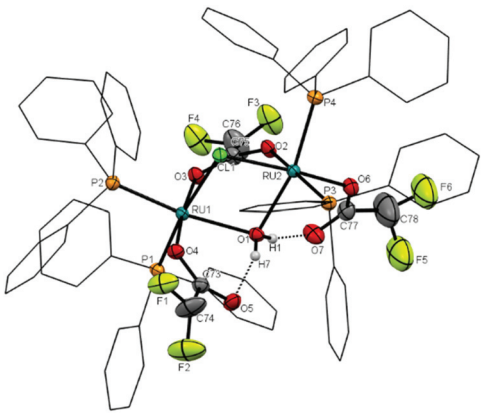

Fig. 3 ORTEP style drawing of the dinuclear complex **3**. Phenyl rings depicted in wireframe style. All hydrogen atoms but for H_2O omitted for clarity. Ru^{II} centers are bridged by DFA, Cl^- and H_2O. Hydrogen bond distances between O7···H1 and O5···H7 are found to be 1.735 and 1.887 Å, respectively.

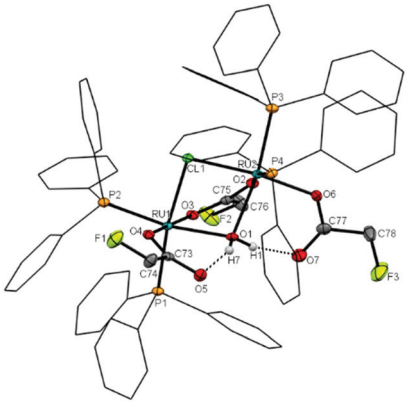

Fig. 4 ORTEP style drawing of the dinuclear complex **4**. Phenyl rings depicted in wireframe style. All hydrogen atoms but for H_2O omitted for clarity. Ru^{II} centers are bridged by MFA, Cl^- and H_2O. Hydrogen bond distances between O7···H1 and O5···H7 are found to be 1.705 and 1.888 Å, respectively.

Table 1 Characteristic bond lengths of complexes **2**, **3** and **4**

Complex	**2**	**3**	**4**
O7···H1, O5···H7 [Å]	1.754, 1.888	1.735, 1.887	1.705, 1.888
Ru1–O4 [Å] (μ1)	2.106(2)	2.097(3)	2.101(3)
Ru2–O6 [Å] (μ1)	2.099(2)	2.101(3)	2.106(3)
Ru1–O3 [Å] (μ2)	2.0947(17)	2.089(3)	2.091(3)
Ru2–O2 [Å] (μ2)	2.1520(17)	2.134(3)	2.136(3)

Based on the dinuclear complex **2**, the mononuclear species **1** is synthesized. Complex **1** is obtained in 45% yield by reacting **2** with TlO_2CCF_3 (1 equiv.) in acetone at room temperature for 2 d (Scheme 2, **I**).

Alternatively, **1** can be prepared from $RuCl_2(PPh_3)_3$, with TlO_2CCF_3 (3 equiv.) in acetone at room temperature for 1 h (Scheme 2, **II**) in 57% yield. Following the latter pathway, the high solubility of **1** in various organic solvents complicates the isolation of **1** as a pure product. Purification of **1** from PPh_3 is finally achieved by concentrating the filtered solution to a minimum amount of acetone and subsequent precipitation by addition of *n*-heptane. The formation of **1** is evidenced by singlets at δ = 54.4 ppm in the ^{31}P NMR spectrum and δ = −75.38 ppm in the ^{19}F NMR spectrum. The liquid injection

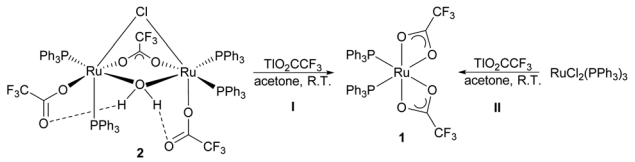

Scheme 2 Synthesis of **1** from dinuclear complex **2** (I) or from $RuCl_2(PPh_3)_3$ (II) in acetone.

field desorption ionization mass spectrum (LIFDI-MS) further confirms the formation of **1** as a mononuclear complex, showing m/z = 851.49, in agreement with the theoretical value of m/z = 852.06. The LIFDI-MS analytical technique was chosen due to its mild ionization in comparison with the electrospray ionization (ESI) technique. Furthermore, the possibility to work under argon atmosphere makes this technique especially useful for sensitive complexes. Upon diffusion of *n*-heptane into a solution of **1** in CH_2Cl_2, crystals of $Ru_2(O_2CCF_3)_4(PPh_3)_4(\mu\text{-}H_2O)$ (**1a**) are obtained. The X-ray structure of **1a** shows a dinuclear complex with two pseudo-octahedrally coordinated ruthenium(II) centers, bridged by two trifluoroacetate ligands and one H_2O molecule (Fig. 5).

Analogous to complexes **2**, **3** and **4**, the dinuclear complex **1a** is stabilized in the solid state by the inclusion of a water molecule. The bridging H_2O is probably incorporated due to the high affinity of the ruthenium trifluoroacetate complexes to water, which originates from moisture remnants in the CH_2Cl_2 used for crystallization. Additional stabilization in the solid state takes place through hydrogen bond formation between the bridging water molecule and the η^1-trifluoroacetate ligands, with both O···H distances measuring 1.761 Å. The Ru–O bond of the trifluoroacetate ligand in *trans* position to PPh_3 is considerably longer than the one in the *trans* position to the η^1-trifluoroacetate (Ru1–O2 = 2.088 Å *vs.* Ru1–O3 = 2.171 Å), as expected from the strong *trans* influence exerted by PPh_3. The structure of **1a** resembles the one reported by Airliguie *et al.* for $[Ru(C_6H_9PCy_2)(CF_3COO)]_2(\mu\text{-}CF_3COO)_2(\mu\text{-}H_2O)$.[24] Crystallization of **1** in anhydrous CH_2Cl_2/*n*-heptane and in the presence of TlO_2CCF_3 yields a mixed complex containing two ruthenium and two thallium atoms $[Ru(O_2CCF_3)_2(PPh_3)_2(TlO_2CCF_3)]_2$ (**1b**) (see the ESI†).

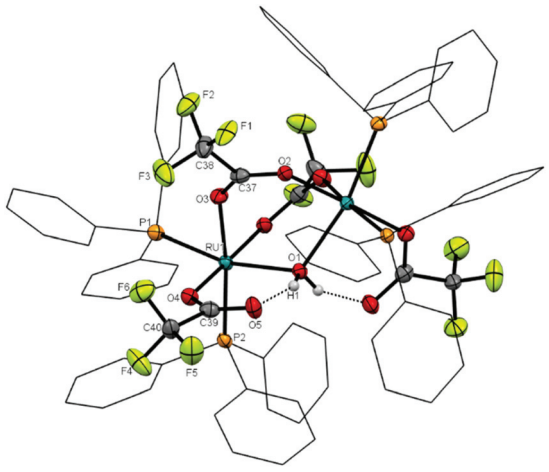

Fig. 5 ORTEP style drawing of the symmetric complex **1a**. Phenyl rings depicted in wireframe style. All hydrogen atoms but for H_2O omitted for clarity. Ru^{II} centers are bridged by two trifluoroacetate ligands and one H_2O molecule. The distance between O5···H1 is found to be 1.761 Å.

Complex **1** shows a high reactivity towards the formation of adducts, especially with water, which strongly interacts with ruthenium and the trifluoroacetate moiety. However, even though structures **1a** and **1b** are obtained in the solid state, NMR measurements clearly confirm that **1** is formed as a mononuclear species without an additional H_2O molecule in solution. Furthermore, only the mass for the monoculear complex and no higher mass signals are detected in the LIFDI-MS, corroborating that the formation of the dinuclear complexes **1a** and **1b** only occurs upon crystallization.

To circumvent the relatively toxic thallium reagent for the synthesis of **1**, AgO_2CCF_3 was examined as an alternative reagent. However, attempts to prepare **1** by reacting $RuCl_2(PPh_3)_3$ with AgO_2CCF_3 in acetone at room temperature, following the procedure of Yamamoto *et al.*,[16] failed. The appearance of two sharp singlets at δ = 56.5 and 17.0 ppm in the ^{31}P NMR spectrum was observed. A color change of the reaction solution from orange to deep purple hints towards side reactions (*e.g.* redox processes) involving silver.

With **1** in hand, the reactivity of this labile complex was examined towards carbon monoxide and free phosphines. Thus, **1** undergoes facile carbonylation under CO (8 bar) in toluene-d_8 at room temperature overnight (eqn (2)). NMR measurements of the resulting carbonyl derivative **5** in toluene-d_8 show a sharp singlet at δ = 30.8 ppm in the ^{31}P NMR spectrum, evidencing the formation of a symmetric species with two *trans* P–P ligands.[41] The ^{13}C spectrum reveals a triplet at δ = 196.6 ppm (^2J(CP) = 10.9 Hz), in accordance with the carbonyl in *cis* position to the phosphorus moieties. IR measurements show two strong carbonyl stretching bands at ν(CO) = 1997 and 2059 cm^{-1}, indicating a *cis* configuration of these two CO ligands. The $\nu(OCO)_{asym}$ = 1684 cm^{-1} evidences a κ^1-binding mode of the trifluoroacetate ligands and thus the substitution of the product with two carbonyl moieties.[42] The data are in accordance with the formation of the thermodynamic dicarbonyl product $Ru(O_2CCF_3)_2(CO)_2(PPh_3)_2$ (**5**), in line with literature data.[43–45]

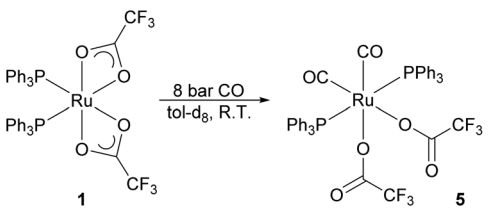

(2)

In order to stabilize **1**, the bidentate 1,4-bis(diphenylphosphino)butane (dppb) was added. The reaction of **1** with dppb (2 equiv.) in CD_2Cl_2 for 1 h at room temperature results in the complete transformation of **1** and the liberation of PPh_3, as

monitored by ^{31}P NMR measurements. Instead of the expected singlet for $Ru(O_2CCF_3)_2$(dppb), which would result from the phosphine exchange of the two PPh_3 ligands of **1** to the bidentate dppb, two broad multiplets at δ = 25.1 and 42.1 ppm are observed in the ^{31}P NMR spectrum. The resulting species could not be isolated, and a structure determination was carried out by SC-XRD. Upon slow diffusion of *n*-pentane to the CD_2Cl_2-solution, single crystals of **6** were formed (Fig. 6). The X-ray structure of **6** shows two ruthenium(II) centers in a pseudo-octahedral coordination geometry, bridged by a dppb ligand, with one dppb and two trifluoroacetate moieties on each ruthenium center. The composition of complex **6** indicates that additional stabilization of the examined trifluoroacetate complexes occurs through the formation of dinuclear species. Furthermore, **6** shows different behavior of the trifluoroacetate- compared to the analogous acetate-complex, the latter yielding $Ru(O_2CCH_3)_2$(dppb) upon reaction with the bidentate phosphine.[46]

Due to the toxicity of thallium reagents and the failure of the silver route, another thallium-free pathway was envisioned for the synthesis of complex **1**. Based on the higher acidity of the fluorinated acetic acids in comparison with acetic acid, the protonation of $Ru(OAc)_2(PPh_3)_2$ with TFA, DFA and MFA to exchange the anion was anticipated (eqn (3)).

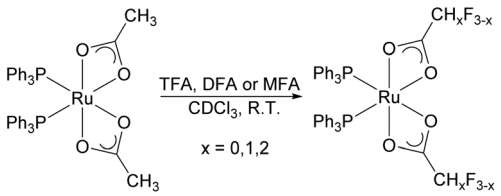

(3)

Addition of trifluoroacetic acid (3–6 equiv.) to $Ru(OAc)_2(PPh_3)_2$ in $CDCl_3$ results in an immediate reaction at room temperature, as inferred by NMR spectroscopy. In the ^{31}P NMR spectrum, the resonance of the starting material at δ = 63.8 ppm disappears and a sharp singlet at δ = 52.6 ppm, attributable to **1**, is observed. In the ^{1}H NMR spectrum, a shift of the acetate CH_3 resonance from δ = 1.51 ppm to 2.12 ppm indicates the elimination of acetic acid, whereas the shift of the CF_3 signal from δ = −76.55 ppm to −75.98 ppm in the ^{19}F NMR spectrum is consistent with the coordination of the trifluoroacetate in **1**. The work-up and isolation of the product failed on account of the high sensitivity of **1** towards H_2O, acids and coordinating solvents (alcohols, ethers), resulting in the formation of several species in the examined solvents, as observed by ^{19}F and ^{31}P NMR measurements.

Protonation of $Ru(OAc)_2(PPh_3)_2$ with the less acidic DFA and MFA gave similar results to those obtained with TFA (eqn (3)), affording the elimination of acetic acid. In the ^{31}P NMR spectra, singlets at δ = 56.8 ppm (DFA) and δ = 55.5 ppm (MFA) evidence the formation of mononuclear species similar to **1** in $CDCl_3$ at room temperature. In the ^{1}H NMR spectra, singlets at δ = 2.15 ppm (DFA) and δ = 2.07 ppm (MFA) are attributed to the release of acetic acid. The isolation of these ruthenium complexes failed, affording a mixture of products.

The high lability of the trifluoroacetate ligands of **1** prompted to attempt the stabilization of this complex by addition of appropriate coordinating ligands. To force the TFA ligands in **1** into a η^1 binding mode, which has been shown to be beneficial for the stabilization of (fluoro-)acetate complexes,[46,47] a chelating ligand was added. Additives like ethyleneglycol and ethylenediamine were chosen due to their ability to coordinate as bidentate ligands. The functional groups, especially the amino group, are further known to enhance the catalytic activity of the respective complexes in hydrogenation reactions of carbonyl compounds,[48–53] beneficial for the catalytic performance of those precursors. In addition, bidentate phosphine ligands, such as dppb, can stabilize ruthenium complexes in comparison with the monodentate PPh_3 analogues. Thus, the stabilized complex **7** is obtained in 78% yield by addition of ethyleneglycol (1 equiv.) to a solution of $Ru(OAc)_2$(dppb) and TFA (3 equiv.) in THF at room temperature for 3 h (eqn (4)).

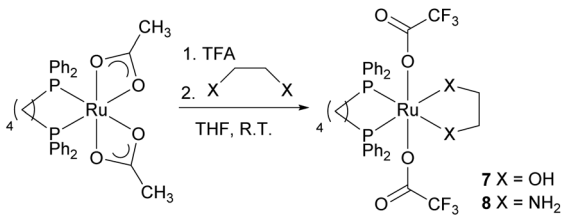

(4)

Single crystals of **7** were obtained by slow diffusion of *n*-pentane to a concentrated solution of **7** in Et_2O. The X-ray crystal structure confirms the formation of **7** in the solid state (Fig. 7), showing the pseudo-octahedral coordination of dppb, ethyleneglycol and two TFA ligands to the ruthenium(II) center. Complex **7** is stabilized by hydrogen bonds between the hydrogen atoms of the ethylene glycol OH-group to the oxygen atoms of the monodentate TFA ligands, with O···H distances of 1.770 Å and 1.796 Å, similar to the water adducts **2–4**.

In the ^{31}P NMR spectrum, **7** exhibits a sharp singlet at δ = 53.0 ppm for the dppb ligand in *trans* position to the glycol ligand, and a singlet at δ = −75.99 ppm in the ^{19}F NMR spectrum. The ^{1}H NMR spectrum of **7** shows a singlet at δ = 9.85 ppm for the two OH protons interacting with the trifluoroacetate ligand by hydrogen bonding. LIFDI-MS

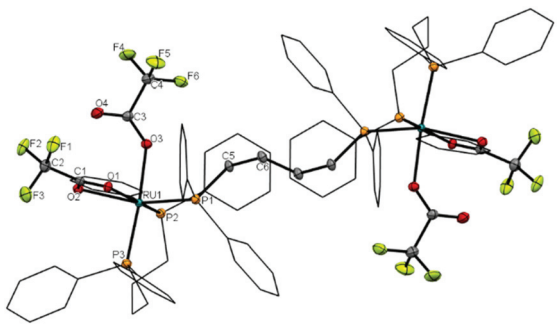

Fig. 6 ORTEP style drawing of the symmetric dinuclear complex **6** formed by the reaction of **1** with 2 equiv. dppb in CD_2Cl_2. Phenyl rings depicted in wireframe style. All hydrogen atoms are omitted for clarity.

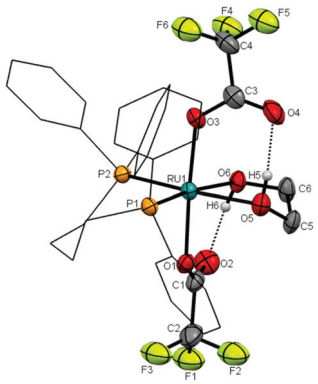

Fig. 7 ORTEP style drawing of complex **7**. Phenyl rings depicted in wire-frame style. All hydrogen atoms but for OH omitted for clarity. Hydrogen bond distances between O2···H6 and O4···H5 are found to be 1.770 and 1.796 Å, respectively.

measurements confirm the formation of **7**, with m/z = 815.59. The NMR and MS studies in solution are in accordance with the crystal structure obtained for **7**.

Complex **8** can be isolated by the reaction of $Ru(OAc)_2$(dppb) and TFA (3 equiv.) with ethylenediamine (1 equiv.) in THF at room temperature in 98% yield (eqn (4)). The crystal structure of **8** shows a pseudo-octahedral coordination of two TFA ligands, ethylenediamine and dppb to the ruthenium(II) center. Complex **8** is additionally stabilized by hydrogen bonds between the oxygen atoms of the TFA ligands and the NH hydrogen atoms of ethylenediamine, with O···H distances of 2.103 Å and 2.145 Å (Fig. 8).

In the ^{31}P NMR spectrum, **8** exhibits a sharp singlet at δ = 43.7 ppm for the dppb ligand in *trans* position to the N ligand, and a singlet at δ = −75.96 ppm in the ^{19}F NMR spectrum. The ^{1}H NMR spectrum of **8** shows a singlet at δ = 4.22 ppm for the four NH protons. LIFDI-MS measurements confirm the formation of **8**, with m/z = 814.17. The

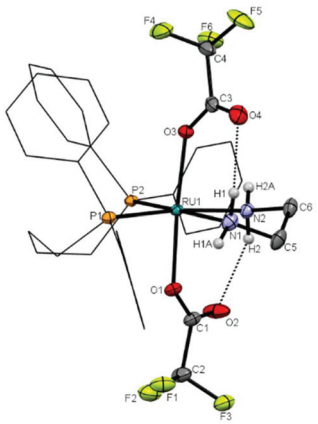

Fig. 8 ORTEP style drawing of complex **8**. Phenyl rings depicted in wire-frame style. All hydrogen atoms but for NH_2 omitted for clarity. Hydrogen bond distances measured between O2···H2 and O4···H1 are 2.103 and 2.145 Å, respectively.

NMR and MS studies are consistent with the X-ray measurements, indicating that **8** exhibits the same structure in solution and in the solid state.

The results indicate that ruthenium fluoroacetate complexes are reactive species displaying a flexible fluoroacetate ligand that can act as a bidentate or monodentate ligand by the addition of O and N donating ligands. OH and NH functionalities are of particular interest for the stabilization of the complexes *via* hydrogen bond formation.

To summarize, the synthesis of ruthenium(II) fluoroacetate phosphine complexes can be accomplished starting from $RuCl_2(PPh_3)_3$ and $NaO_2CH_xCF_{3-x}$ (x = 0, 1, 2) *via* different pathways to achieve the dinuclear species **2**, **3** and **4** (Scheme 3). The reaction of TlO_2CCF_3 with $RuCl_2(PPh_3)_3$ or with the dinuclear species **2** leads to the highly dynamic complex **1** with labile trifluoroacetate ligands. Complex **1** can easily react with water, CO and the diphosphine dppb (Scheme 3). Trifluoroacetate complexes are also obtained from $Ru(OAc)_2$(dppb) as precursor and TFA in the presence of ethyleneglycol and ethylenediamine, affording complexes **7** and **8**. With the successfully synthesized ruthenium(II) trifluoroacetates **1**, **7** and **8** in hand, examinations of these catalyst precursors in the transfer hydrogenation of ketones were carried out. Furthermore, comparison of the dinuclear complexes **2**, **3** and **4** in the catalytic transfer hydrogenation was attempted.

Catalytic transfer hydrogenation of ketones

The catalytic activities of complexes **1–4** and **7**, **8** were examined in the transfer hydrogenation (TH)[54–58] of aromatic and aliphatic ketones in ^{i}PrOH as hydrogen donor with NaO^{i}Pr as base (eqn (5)).

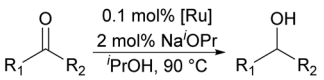

(5)

Complex **1** (0.1 mol%) displays poor catalytic activity in the TH of acetophenone with 21% conversion to 2-phenylethanol in 48 h in the presence of Na^{i}OPr (2 mol%). The dinuclear complexes **2–4** (0.05 mol%) show up to 50% conversion of acetophenone to 2-phenylethanol in 7 h in the presence of Na^{i}OPr (2 mol%), with TOFs of up to 75 h^{-1} (calculated at 50% conversion of acetophenone). The low catalytic activity of **1–4** can be attributed to catalyst instability. When **1** and **2–4** are dissolved in ^{i}PrOH and kept at room temperature overnight or at 60 °C for 1 h, respectively, a color change from orange to pink and turquoise was observed, suggesting catalyst decomposition.

Complexes **7** and **8**, bearing a bidentate phosphine dppb and bidentate O and N ligands, display a higher catalytic activity in the ketone TH. Acetophenone can easily be reduced with **7** and **8** (78% and 97% conversion) with TOFs of 5000 h^{-1} and 4200 h^{-1}, respectively (Table 2, entries 1 and 2).

Despite its higher TOF, the glycol-containing complex **7** only reaches a maximum of 78% conversion, indicating a facile formation of the active species, but a lower stability than its amine analogue **8**. These results prompted further examin-

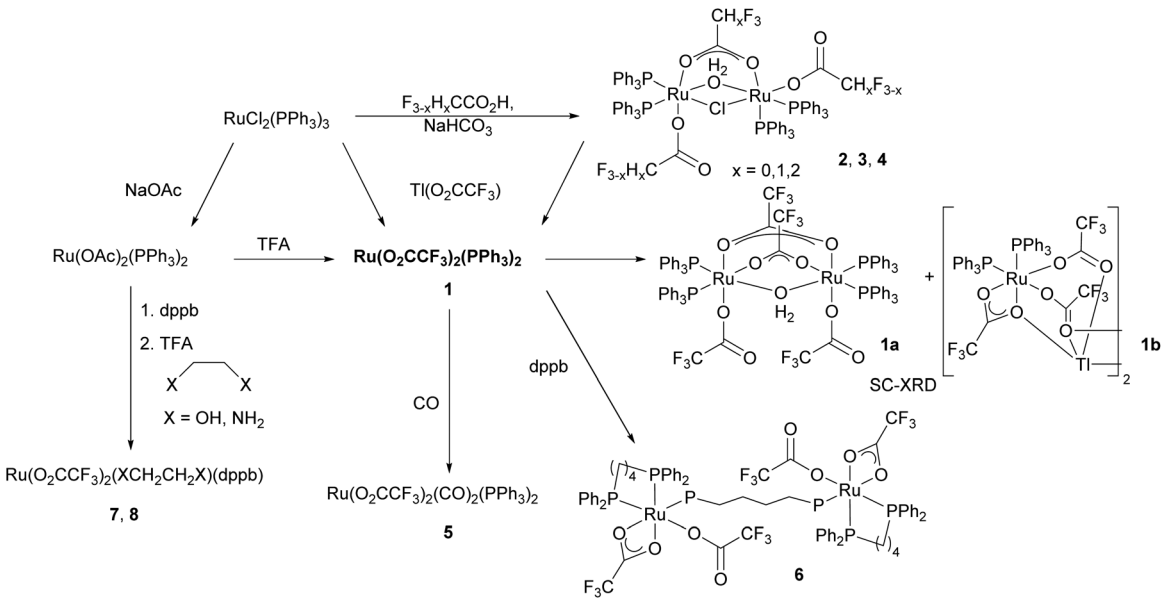

Scheme 3 Ruthenium(II) trifluoroacetate complexes synthesized in this work.

Table 2 Transfer hydrogenation of ketones in ^{i}PrOH at 90 °C with NaO^{i}Pr as base[a]

Entry	Substrate	Catalyst	Catalyst loading [mol%]	Time [min]	Conversion [%]	TOF[b] [h^{-1}]
1		**7**	0.1	480	78	5000
2		**8**	0.1	30	97	4200
3	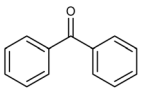	**7**	0.1	480	45	60
4		**8**	0.1	480	78	1900
5	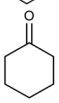	**7**	0.1	5	100	15 000
6		**8**	0.1	40	100	4100
7		**7**	0.03	240	82	22 000
8		**8**	0.03	1500	69	1700

[a] S : B = 1000 : 20. [b] Calculated at 50% conversion.

ations of the influence of the NH_2 group of the ethylenediamine ligand in comparison with the OH of ethyleneglycol on the catalytic activity of the complexes.[50,52] In the TH of benzophenone (Table 2, entries 3 and 4), the amine catalyst **8** shows a higher activity with respect to the glycol derivative **7** (TOF = 1900 h^{-1} *vs.* 60 h^{-1}, respectively). Conversely, cyclohexanone was reduced quantitatively to cyclohexanol in 5 min with **7** (0.1 mol%), whereas **8** required 40 min, affording TOFs of 15 000 h^{-1} and 4100 h^{-1}, respectively (Table 2, entries 5 and 6). At a lower catalyst loading of **7** and **8** (0.03 mol%), up to 82% and 69% conversion were obtained, with TOFs of 22 000 h^{-1} and 1700 h^{-1} (Table 2, entries 7 and 8). The results indicate that ethyleneglycol can be used as a suitable ligand for ruthenium diphosphine catalysts, affording a superior accelerating effect with respect to the well-known ethylenediamine ligand in the reduction of the aliphatic cyclohexanone.

In summary, complexes **1–4** and **7** and **8** are active catalysts in the transfer hydrogenation of aromatic and aliphatic ketones. While derivatives **1–4** show a low catalytic activity, presumably due to their instability under the applied conditions, compounds **7** and **8** exhibit good catalytic properties. For the aliphatic substrate cyclohexanone, the glycol derivative **7** displays a higher activity compared to the diamine complex **8**, with TOFs up to 22 000 h^{-1}.

Conclusions

Ruthenium(II) phosphine complexes bearing mono-, di- and trifluoroacetato ligands have been isolated and characterized in solution and in the solid state. The complexes have been synthesized starting from $RuCl_2(PPh_3)_3$ *via* substitution reactions or from $Ru(OAc)_2$(dppb) by protonation with fluoroacetic acids. The presence of weakly coordinating fluoroacetate ligands affords reactive ruthenium complexes, which are stabilized by water, glycol and amine ligands, and are

soluble in a variety of organic solvents. Isolation of $Ru(O_2CCF_3)_2(PPh_3)_2$ (**1**) is reported for the first time, correcting the former preparation, where the dinuclear complex $Ru_2Cl(O_2CCF_3)_3(PPh_3)_4(\mu\text{-}H_2O)$ (**2**) had been obtained instead. Complex **2** is stabilized by hydrogen bonds between the bridging water and the trifluoroacetate ligands. Preliminary studies show that the ruthenium triphenylphosphine fluoroacetate derivatives exhibit rather poor activity in ketone transfer hydrogenation reactions with 2-propanol, whereas the dppb complexes **7** and **8**, which are additionally stabilized by ethyleneglycol and ethylenediamine, display much better catalytic activities. The best performance is achieved with the glycol derivative **7** in the reduction of cyclohexanone (TOFs up to 22 000 h^{-1}). Studies to extend the use of these reactive precursors and their application in catalysis are currently in progress.

Experimental

General

All reactions were carried out under argon atmosphere using standard Schlenk techniques. Solvents were used after distillation or taken from a solvent purification system (SPS) from MBraun (THF), degassed and stored over molar sieves (3 and 4 Å). Ruthenium precursors were obtained from Johnson Matthey Ltd and all other chemicals were purchased from Sigma Aldrich, Merck and abcr. $Ru(OAc)_2$(dppb) was prepared following a literature procedure.[46] TlO_2CCF_3 was synthesized by reacting $Tl_2(CO_3)$ with an excess of TFA and subsequent drying under vacuum. NMR measurements were performed on Bruker AV-500 cr and AC-200 instruments. Chemical shifts in ppm are reported relative to the stated solvent for ^1H and $^{13}C\{^1H\}$ spectra, relative to H_3PO_4 for $^{31}P\{^1H\}$ spectra, and relative to CF_3COOH for ^{19}F and $^{19}F\{^1H\}$ experiments. Elemental analyses (C, H, N) were carried out on a Varian SpectrAA-400 instrument and on a Flash EA1112 elemental analyzer from Carlo Erba. GC analyses were performed on Varian CP-3380/Agilent 7890B gas chromatographs equipped with a MEGADEX-ETTBDMS-β chiral column of 25 m length/an HP-5 column with 30 m length, column pressure 5 psi, H_2/Ar as carrier gases, and a flame ionization detector (FID). The injector and detector temperatures were 250 °C/300 °C, with initial T = 95 °C/80 °C ramped to 140 °C at 3 °C min^{-1}/138 °C at 8 °C min^{-1} and then to 210 °C at 20 °C min^{-1}/300 °C at 30 °C min^{-1}. Infrared (IR) spectra were collected on a Mettler-Toledo react-IR 45 m spectrometer equipped with a Sentinel/Si-Comp probe and a Mercury Cadmium Telluride (MCT) detector. Samples for mass spectra (MS) measurements were dissolved in CH_2Cl_2, filtered through a syringe filter and sealed with a Teflon cap under argon atmosphere. The spectra were recorded on a Waters LCT device equipped with a liquid injection field desorption ionization (LIFDI) source under an air free atmosphere to enable measurements of air-sensitive compounds. Sample introduction was carried out by withdrawing the solution from the closed vessel through the septum with a glass capillary under reduced pressure. The sample solution is transmitted to a tungsten wire coated with thousands of micro-graphite dendrites. The sample is distributed over the emitter and the employed solvent is evaporated in the prevacuum of the mass spectrometer. A potential of 5 kV is applied between the emitter and the counter electrode in order to ionize and accelerate the sample molecules to the counter electrode and then to the argon-flushed detector. In order to increase the mobility of the molecules on the emitter, an electrical current ramp of 30 mA min^{-1} is applied through the tungsten wire.

Synthesis of $Ru(O_2CCF_3)_2(PPh_3)_2$ (1)

From complex 2. A suspension of 100 mg **2** (1 equiv., 0.061 mmol) and 23.2 mg TlO_2CCF_3 (1.2 equiv., 0.073 mmol) in 1 mL acetone is stirred at room temperature for 2 d and then filtered under argon. The filtrate is stripped to a minimum amount of acetone and the product is precipitated in *n*-heptane. Drying under vacuum affords 46.6 mg of the product (45% yield). El. Anal. Calcd for $C_{40}H_{30}F_6O_4P_2Ru$: C, 56.41; H, 3.55. Found: C, 56.19; H, 4.14. MS (LIFDI, *m*/*z*): calc. for $C_{40}H_{30}F_6O_4P_2Ru$: 852.0579; found: 851.4905 $[M]^-$. ^1H-NMR (500 MHz, CD_2Cl_2, 293 K): δ (ppm) = 6.14–7.88 (m, 30H, aromatic protons). $^{13}C\{^1H\}$-NMR (126 MHz, CD_2Cl_2, 293 K): δ (ppm) = 168.2 (q, ^2J(CF) = 38.3 Hz, O_2CCF_3), 133.9–135.0 (m, aromatic carbon atoms), 130.2 (s, aromatic carbon atoms), 127.8–128.4 (m, aromatic carbon atoms), 104.5–120.4 (m, O_2CCF_3). $^{19}F\{^1H\}$-NMR (471 MHz, CD_2Cl_2, 293 K): δ (ppm) = −75.38 (s). $^{31}P\{^1H\}$-NMR (203 MHz, CD_2Cl_2, 293 K): δ (ppm) = 54.4 (s).

From $RuCl_2(PPh_3)_3$. A suspension of 100 mg $RuCl_2(PPh_3)_3$ (1 equiv., 0.104 mmol) and 99.3 mg TlO_2CCF_3 (3 equiv., 0.313 mmol) in 1 mL acetone is stirred at room temperature for 1 h and then filtered under argon. The filtrate is stripped to a minimum amount of acetone and the product is precipitated and washed with *n*-heptane (4 × 0.5 mL). Drying under vacuum affords 50.5 mg of the product (57% yield).

General procedure for the synthesis of dinuclear fluoroacetate complexes 2–4

To a suspension of $RuCl_2(PPh_3)_3$ (1 equiv., 100 mg, 0.104 mmol) and $NaHCO_3$ (4 equiv., 35 mg, 0.417 mmol) in 6 mL ^{t}BuOH, the respective fluoroacetic acid (5 equiv., 0.521 mmol) is added. The mixture is heated to 90 °C for 3 h and then cooled to room temperature. The orange precipitate is filtered under argon, washed with H_2O (4 × 1 mL), MeOH (2 × 1 mL) and Et_2O (1 × 0.5 mL) and dried under vacuum.

Crystals for SC-XRD measurements were obtained by diffusion of *n*-pentane to a solution of the ruthenium complex in dichloromethane.

$Ru_2Cl(O_2CCF_3)_3(PPh_3)_4(\mu\text{-}H_2O)$ (2). The orange product **2** was obtained in 85% yield (72.9 mg). El. Anal. Calcd for $C_{78}H_{62}ClF_9O_7P_4Ru_2$: C, 56.99; H, 3.80. Found: C, 57.05; H, 3.25. ^1H-NMR (200 MHz, CD_2Cl_2, 293 K): δ (ppm) = 9.51 (s, 2H, H_2O), 8.25–6.29 (m, 60H, aromatic protons). $^{13}C\{^1H\}$-NMR (50 MHz, CD_2Cl_2, 293 K): δ (ppm) = 166.0–167.5 (m, O_2CCF_3), 122.5–138.8 (m, aromatic carbon atoms), 99.9–116.4 (m,

O_2CCF_3). $^{19}F\{^1H\}$-NMR (188 MHz, CD_2Cl_2, 293 K): δ (ppm) = −74.52 (s, 3F), −74.60 (s, 3F), −76.70 (s, 3F). $^{31}P\{^1H\}$-NMR (81 MHz, CD_2Cl_2, 293 K): δ (ppm) = 50.9 (d, ^2J(PP) = 42.1 Hz), 50.3 (d, ^2J(PP) = 42.1 Hz), 48.7 (d, ^2J(PP) = 38.9 Hz), 47.7 (d, ^2J(PP) = 38.8 Hz).

$Ru_2Cl(O_2CCHF_2)_3(PPh_3)_4(\mu\text{-}H_2O)$ (3). The orange product **3** was obtained in 42% yield (34.2 mg). El. Anal. Calcd for $C_{81}H_{71}ClF_6O_7P_4Ru_2$: C, 58.93; H, 4.12. Found: C, 58.64; H, 4.09. ^{1}H-NMR (500 MHz, $CDCl_3$, 293 K): δ (ppm) = 10.34 (br s, 2H, H_2O), 6.25–7.89 (m, 60H, aromatic protons), 5.13 (t, ^2J(HF) = 55.0 Hz, 1H, CHF_2), 5.10 (t, ^2J(HF) = 55.0 Hz, 1H, CHF_2), 4.75 (t, ^2J(HF) = 55.0 Hz, 1H, CHF_2). $^{13}C\{^1H\}$-NMR (126 MHz, $CDCl_3$, 293 K): δ (ppm) = 172.7–174.7 (m, O_2CCHF_2), 123.4–138.2 (m, aromatic carbon atoms), 107.3 (t, ^1J(CF) = 250.2 Hz, O_2CCHF_2), 106.7 (t, ^1J(CF) = 250.2 Hz, O_2CCHF_2). $^{19}F\{^1H\}$-NMR (471 MHz, $CDCl_3$, 293 K): δ (ppm) = −124.08 (s, 1F), −124.32 (s, 1F), −124.33 (s, 1F), −124.88 (s, 2F), −125.25 (s, 1F). ^{19}F-NMR (471 MHz, $CDCl_3$, 293 K): δ (ppm) = −124.08 (d, ^2J(HF) = 55.0 Hz), −124.27 (d, ^2J(HF) = 55.0 Hz), −124.38 (d, ^2J(HF) = 55.0 Hz), −124.88 (d, ^2J(HF) = 55.0 Hz), −125.25 (d, ^2J(HF) = 55.0 Hz). $^{31}P\{^1H\}$-NMR (203 MHz, $CDCl_3$, 293 K): δ (ppm) = 51.8 (d, ^2J(PP) = 40.6 Hz), 49.7 (d, ^2J(PP) = 40.6 Hz), 49.2 (d, ^2J(PP) = 40.6 Hz), 48.3 (d, ^2J(PP) = 40.6 Hz).

$Ru_2Cl(O_2CCH_2F)_3(PPh_3)_4(\mu\text{-}H_2O)$ (4). The orange product **4** was obtained in 51% yield (49.5 mg). El. Anal. Calcd for $C_{78}H_{68}ClF_3O_7P_4Ru_2$: C, 61.00; H, 4.46. Found: C, 60.60; H, 3.85. ^{1}H-NMR (200 MHz, CD_2Cl_2, 293 K): δ (ppm) = 10.19 (br s, 2H, H_2O), 6.35–7.95 (m, 60H, aromatic protons), 4.17 (d, ^2J(HF) = 48.8 Hz, 2H, CH_2F), 4.06 (d, ^2J(HF) = 48.8 Hz, 2H, CH_2F), 3.44–4.40 (m, 2H, CH_2F). $^{13}C\{^1H\}$-NMR (50 MHz, CD_2Cl_2, 293 K): δ (ppm) = 171.6–181.9 (m, O_2CCH_2F), 120.2–142.7 (m, aromatic carbon atoms), 79.9 (d, ^1J(CF) = 184.4 Hz, O_2CCH_2F), 79.8 (d, ^1J(CF) = 184.9 Hz, O_2CCH_2F), 79.5 (d, ^1J(CF) = 182.6 Hz, O_2CCH_2F). $^{19}F\{^1H\}$-NMR (188 MHz, CD_2Cl_2, 293 K): δ (ppm) = −216.38 (s, 1F), −218.43 (s, 1F), −218.89 (s, 1F). ^{19}F-NMR (188 MHz, CD_2Cl_2, 293 K): δ (ppm) = −216.38 (t, ^2J(HF) = 48.8 Hz), −218.43 (t, ^2J(HF) = 48.8 Hz), −218.89 (t, ^2J(HF) = 48.8 Hz). $^{31}P\{^1H\}$-NMR (81 MHz, CD_2Cl_2, 293 K): δ (ppm) = 53.5 (d, ^2J(PP) = 38.9 Hz), 50.5 (d, ^2J(PP) = 42.8 Hz), 50.5 (d, ^2J(PP) = 36.5 Hz), 49.7 (d, ^2J(PP) = 40.1 Hz).

Spectral evidence for $Ru(O_2CCF_3)_2(CO)_2(PPh_3)_2$ (5)

A solution of 10 mg **1** (1 equiv., 0.012 mmol) in 0.45 mL toluene-d_8 is subjected to 8 bar CO in a high-pressure NMR tube and the mixture is reacted overnight. The colorless solution is then analyzed by NMR and IR spectroscopy. ^{1}H-NMR (200 MHz, tol-d_8, 293 K): δ (ppm) = 7.91–7.71 (m, 12H, aromatic protons), 7.61 (ddd, ^3J(HH) = 12.01 Hz, ^4J(HH) = 7.97 Hz, ^5J(HH) = 1.68 Hz, 2H, aromatic protons), 7.39–7.23 (m, 4H, aromatic protons), 7.13–7.04 (m, 12H, aromatic protons). $^{13}C\{^1H\}$-NMR (101 MHz, tol-d_8, 293 K): δ (ppm) = 196.6 (t, ^2J(CP) = 10.9 Hz, CO), 162.0 (q, ^2J(CF) = 37.2 Hz, O_2CCF_3), 116.0 (q, ^1J(CF) = 290.1 Hz, O_2CCF_3), 138.2–135.8 (m, aromatic carbon atoms), 134.6–133.6 (m, aromatic carbon atoms), 129.6–128.7 (m, aromatic carbon atoms). $^{19}F\{^1H\}$-NMR (471 MHz, tol-d_8, 293 K): δ (ppm) = −73.71. $^{31}P\{^1H\}$-NMR (162 MHz, tol-d_8, 293 K): δ (ppm) = 30.8 (s). IR (tol-d_8): ν (cm^{-1}) = 2059 ($CO_{stretch}$), 1997 ($CO_{stretch}$), 1684 (OCO_{asym}).

Synthesis of $Ru(O_2CCF_3)_2(dppb)(HOCH_2CH_2OH)$ (7)

To a suspension of $Ru(OAc)_2$(dppb) (1 equiv., 100 mg, 0.155 mmol) in THF, 3 equiv. TFA (36 μL, 0.465 mmol) are added. After stirring at 30 °C for 5 min, a spatula of $CaCO_3$ is added to the resulting solution to precipitate $Ca(OAc)_2$, and the mixture is stirred for another 2 h at 30 °C. Ethyleneglycol is added (1 equiv., 8.7 μL, 0.310 mmol) and the suspension is stirred for another 3 h. After filtration from $Ca(OAc)_2$ under argon, the solution is dried under vacuum to afford 98.8 mg of the orange product (78% yield). El. Anal. Calcd for $C_{34}H_{34}F_6O_6P_2Ru$: C, 50.07; H, 4.20. Found: C, 50.45; H, 3.85. MS (LIFDI, *m*/*z*): calc. for $C_{34}H_{34}F_6O_6P_2Ru$: 816.0778; found: 815.5901 $[M]^-$. ^{1}H-NMR (200 MHz, CD_2Cl_2, 293 K): δ (ppm) = 9.85 (s, 2H, OH), 6.46–8.14 (m, 20H, aromatic protons), 3.63 (s, 4H, $HOCH_2CH_2OH$), 2.12–2.89 (m, 4H, CH_2CH_2P), 1.37–1.87 (m, 4H, CH_2CH_2P). $^{13}C\{^1H\}$-NMR (101 MHz, $CDCl_3$, 293 K): δ (ppm) = 168.7 (q, ^2J(CF) = 37.6 Hz, O_2CCF_3), 132.9 (t, ^1J(CP) = 4.5 Hz, aromatic carbon atoms), 129.9 (s, aromatic carbon atoms), 128.1 (t, ^2J(CP) = 4.7 Hz, aromatic carbon atoms), 113.4 (dd, ^1J(CF) = 578.2 Hz, 289.3 Hz, O_2CCF_3), 64.9 (s, $HOCH_2CH_2OH$), 26.5–28.28 (m, CH_2CH_2P), 22.7 (s, CH_2CH_2P). $^{19}F\{^1H\}$-NMR (471 MHz, $CDCl_3$, 293 K): δ (ppm) = −75.99 (s, 6F). $^{31}P\{^1H\}$-NMR (162 MHz, $CDCl_3$, 293 K): δ (ppm) = 53.0 (s).

Synthesis of $Ru(O_2CCF_3)_2(dppb)(H_2NCH_2CH_2NH_2)$ (8)

To a suspension of $Ru(OAc)_2$(dppb) (1 equiv., 200 mg, 0.310 mmol) in THF, 3 equiv. TFA (72 μL, 0.929 mmol) are added. After stirring at 30 °C for 5 min, a spatula of $CaCO_3$ is added to the resulting solution to precipitate $Ca(OAc)_2$, and the mixture is stirred for another 2 h at 30 °C. Ethylenediamine is added (1 equiv., 21 μL, 0.310 mmol) and the suspension is stirred for another 3 h. After filtration from $Ca(OAc)_2$ under argon, the solution is dried under vacuum to afford 247.0 mg of the orange product (98% yield). El. Anal. Calcd for $C_{34}H_{36}F_6N_2O_4P_2Ru$: C, 50.19; H, 4.46; N, 3.44. Found: C, 51.49; H, 4.53; N, 2.44. MS (LIFDI, *m*/*z*): calc. for $C_{34}H_{36}F_6N_2O_4P_2Ru$: 814.1098; found: 814.1747 $[M]^-$. ^{1}H-NMR (500 MHz, CD_2Cl_2, 293 K): δ (ppm) = 6.46–7.86 (m, 20H, aromatic protons), 4.22 (s, 4H, NH_2), 2.65 (s, 4H, $H_2NCH_2CH_2NH_2$), 2.44–2.56 (m, 4H, CH_2CH_2P), 1.52–1.72 (m, 4H, CH_2CH_2P). $^{13}C\{^1H\}$-NMR (126 MHz, CD_2Cl_2, 293 K): δ (ppm) = 166.2 (q, ^2J(CF) = 35.8 Hz, O_2CCF_3), 132.9 (t, ^1J(CP) = 4.6 Hz, s, aromatic carbon atoms), 129.7 (s, aromatic carbon atoms), 128.4 (t, ^2J(CP) = 4.3 Hz, s, aromatic carbon atoms), 113.8 (q, ^1J(CF) = 291.5 Hz, O_2CCF_3), 44.6 (s, $H_2NCH_2CH_2NH_2$), 23.8–25.3 (m, CH_2CH_2P), 22.3 (s, CH_2CH_2P). $^{19}F\{^1H\}$-NMR (471 MHz, CD_2Cl_2, 293 K): δ (ppm) = −75.96 (s, 6F). $^{31}P\{^1H\}$-NMR (203 MHz, CD_2Cl_2, 293 K): δ (ppm) = 43.8 (s).

Procedure for the catalytic transfer hydrogenation of ketones

Ruthenium mononuclear (1.0 μmol) or dinuclear complexes (0.5 μmol) are dissolved in 10 mL dry and degassed ^{i}PrOH. The ketone substrate (1 mmol) is dissolved in dry and

degassed ^{i}PrOH, and the solution is heated to 90 °C under argon. After addition of 1.0 mL of the catalyst solution and 200 μL NaO^{i}Pr in dry and degassed ^{i}PrOH (0.1 M; 0.02 mmol), the reduction of the ketone starts immediately (final volume of the solution 10 mL). The reaction is sampled by removing an aliquot of the reaction mixture to which diethyl ether is added (1/1, v/v). The solution is filtered over a short silica pad and subsequently the conversion is determined by GC analysis (Ru 0.1 mol%, NaO^{i}Pr 2 mol%, and acetophenone 0.1 M).

Conflicts of interest

There are no conflicts to declare.

Acknowledgements

The authors thank Prof. Janos Mink for discussions on the IR spectra and Dr Paolo Martinuzzi, Benjamin Hofmann and Sebastian Hölzl for NMR, IR and MS measurements. The TUM Graduate Schools of Chemistry and MSE are gratefully acknowledged for financial support for D. A. H. and P. J. F.

Notes and references

1 P. Dupau, P. Le Gendre, C. Bruneau and P. H. Dixneuf, *Synlett*, 1999, 1832–1834.
2 B. Heiser, E. A. Broger and Y. Crameri, *Tetrahedron: Asymmetry*, 1991, **2**, 51–62.
3 P. Le Gendre, F. Jérôme, C. Bruneau and P. H. Dixneuf, *Chem. Commun.*, 1998, **5**, 533–534.
4 P. J. Pye, K. Rossen, R. A. Reamer, R. P. Volante and P. J. Reider, *Tetrahedron Lett.*, 1998, **39**, 4441–4444.
5 N. C. Zanetti, F. Spindler, J. Spencer, A. Togni and G. Rihs, *Organometallics*, 1996, **15**, 860–866.
6 W. Baratta, M. Ballico, A. Del Zotto, E. Herdtweck, S. Magnolia, R. Peloso, K. Siega, M. Toniutti, E. Zangrando and P. Rigo, *Organometallics*, 2009, **28**, 4421–4430.
7 P. Dupau, L. Bonomo and L. Kermorvan, *Angew. Chem., Int. Ed.*, 2013, **52**, 11347–11350.
8 M. Kitamura, M. Tokunaga and R. Noyori, *J. Org. Chem.*, 1992, **57**, 4053–4054.
9 M. Kitamura, M. Tsukamoto, Y. Bessho, M. Yoshimura, U. Kobs, M. Widhalm and R. Noyori, *J. Am. Chem. Soc.*, 2002, **124**, 6649–6667.
10 M. Naruto and S. Saito, *Nat. Commun.*, 2015, **6**, 8140.
11 X. Tan, G. Wang, Z. Zhu, C. Ren, J. Zhou, H. Lv, X. Zhang, L. W. Chung, L. Zhang and X. Zhang, *Org. Lett.*, 2016, **18**, 1518–1521.
12 M. Yoshimura, Y. Ishibashi, K. Miyata, Y. Bessho, M. Tsukamoto and M. Kitamura, *Tetrahedron*, 2007, **63**, 11399–11409.
13 A. Dobson and S. D. Robinson, *J. Organomet. Chem.*, 1975, **87**, C52–C53.
14 R. A. Sanchez-Delgado, J. S. Bradley and G. Wilkinson, *J. Chem. Soc., Dalton Trans.*, 1976, 399–404.
15 A. Dobson and S. D. Robinson, *Inorg. Chem.*, 1977, **16**, 137–142.
16 K. Yamamoto, M. Takagi and J. Tsuji, *Bull. Chem. Soc. Jpn.*, 1988, **61**, 319–321.
17 E. B. Boyar, A. Dobson, S. D. Robinson, B. L. Haymore and J. C. Huffman, *J. Chem. Soc., Dalton Trans.*, 1985, **4**, 621–627.
18 J. Gotzig, R. Werner and H. Werner, *J. Organomet. Chem.*, 1985, **290**, 99–114.
19 R. A. Sanchez-Delgado, N. Valencia, R. Marquez-Silva, A. Andriollo and M. Medina, *Inorg. Chem.*, 1986, **25**, 1106–1111.
20 M. O. Albers, D. C. Liles and E. Singleton, *Acta Crystallogr., Sect. C: Cryst. Struct. Commun.*, 1987, **43**, 860–863.
21 T. Arliguie and B. Chaudret, *Chem. Commun.*, 1989, **3**, 155–157.
22 P. Sarkhel, S. C. Sarker, A. K. Gupta and R. K. Poddar, *Transition Met. Chem.*, 1996, **21**, 250–253.
23 P. González-Herrero, B. Weberndörfer, K. Ilg, J. Wolf and H. Werner, *Angew. Chem., Int. Ed.*, 2000, **39**, 3266–3269.
24 T. Arliguie, B. Chaudret, G. Chung and F. Dahan, *Organometallics*, 1991, **10**, 2973–2977.
25 L. Bonomo, P. Dupau and S. Bonnaudet, *Switzerland Pat.*, WO2011/145032A2, 2011.
26 M. O. Albers, D. C. Liles, E. Singleton and J. E. Yates, *J. Organomet. Chem.*, 1984, **272**, C62–C66.
27 I. Appleby, L. T. Boulton, C. J. Cobley, C. Hill, M. L. Hughes, P. D. de Koning, I. C. Lennon, C. Praquin, J. A. Ramsden, H. J. Samuel and N. Willis, *Org. Lett.*, 2005, **7**, 1931–1934.
28 A. Bartoszewicz, N. Ahlsten and B. Martín-Matute, *Chem. – Eur. J.*, 2013, **19**, 7274–7302.
29 F. Shibahara and M. J. Krische, *Chem. Lett.*, 2008, **37**, 1102–1107.
30 R. Figliolia, S. Baldino, H. G. Nedden, A. Zanotti-Gerosa and W. Baratta, *Chem. – Eur. J.*, 2017, **23**, 14416–14419.
31 H. Werner, G. Fries and B. Weberndörfer, *J. Organomet. Chem.*, 2000, **607**, 182–193.
32 T. G. Appleton, H. C. Clark and L. E. Manzer, *Coord. Chem. Rev.*, 1973, **10**, 335–422.
33 J. P. Collman, L. G. Hegedus, J. R. Norton and R. G. Finke, *Principles and Applications of Organotransition Metal Chemistry*, Oxford University Press, Oxford, 1987.
34 J. C. Toledo, B. dos Santos Lima Neto and D. W. Franco, *Coord. Chem. Rev.*, 2005, **249**, 419–431.
35 T. Steiner, *Angew. Chem., Int. Ed.*, 2002, **41**, 48–76.
36 L. Brammer, *Dalton Trans.*, 2003, 3145–3157.
37 J. van Buijtenen, J. Meuldijk, J. A. J. M. Vekemans, L. A. Hulshof, H. Kooijman and A. L. Spek, *Organometallics*, 2006, **25**, 873–881.
38 T. Funaioli, C. Cavazza, F. Marchetti and G. Fachinetti, *Inorg. Chem.*, 1999, **38**, 3361–3368.

39 Y. Sun, H.-S. Chan, P. H. Dixneuf and Z. Xie, *J. Organomet. Chem.*, 2006, **691**, 3071–3082.
40 Elemental analysis given in ref. 14: C, 56.9; H, 3.8; F, 10.6; P, 7.4, while the calculated values for **1** are, C, 56.4; H, 3.5; F, 13.4; P, 7.3, and for **2**, C, 57.0; H, 3.8; F, 10.4; P, 7.5.
41 L. Pardatscher, M. J. Bitzer, C. Jandl, J. W. Kück, R. M. Reich, F. E. Kühn and W. Baratta, *Dalton Trans.*, 2019, 79–89.
42 M. Nara, H. Torii and M. Tasumi, *J. Phys. Chem.*, 1996, **100**, 19812–19817.
43 A. Dobson, S. D. Robinson and M. F. Uttley, *J. Chem. Soc., Dalton Trans.*, 1975, **5**, 370–377.
44 T. A. Stephenson and G. Wilkinson, *J. Inorg. Nucl. Chem.*, 1966, **28**, 945–956.
45 E. W. Evans, M. B. H. Howlader and M. T. Atlay, *Inorg. Chim. Acta*, 1995, **230**, 193–197.
46 W.-K. Wong, K.-K. Lai, M.-S. Tse, M.-C. Tse, J.-X. Gao, W.-T. Wong and S. Chan, *Polyhedron*, 1994, **13**, 2751–2762.
47 G. Jia, A. L. Rheingold, B. S. Haggerty and D. W. Meek, *Inorg. Chem.*, 1992, **31**, 900–904.
48 D. A. Hey, R. M. Reich, W. Baratta and F. E. Kühn, *Coord. Chem. Rev.*, 2018, **374**, 114–132.
49 R. Noyori, M. Yamakawa and S. Hashiguchi, *J. Org. Chem.*, 2001, **66**, 7931–7944.
50 E. Peris, *Chem. Rev.*, 2018, **118**, 9988–10031.
51 J. Witt, A. Pöthig, F. E. Kühn and W. Baratta, *Organometallics*, 2013, **32**, 4042–4045.
52 B. Zhao, Z. Han and K. Ding, *Angew. Chem., Int. Ed.*, 2013, **52**, 4744–4788.
53 W. Baratta, S. Baldino, M. J. Calhorda, P. J. Costa, G. Esposito, E. Herdtweck, S. Magnolia, C. Mealli, A. Messaoudi, S. A. Mason and L. F. Veiros, *Chem. – Eur. J.*, 2014, **20**, 13603–13617.
54 W. Baratta and P. Rigo, *Eur. J. Inorg. Chem.*, 2008, **26**, 4041–4053.
55 G. Chelucci, S. Baldino and W. Baratta, *Coord. Chem. Rev.*, 2015, **300**, 29–85.
56 F. Foubelo and M. Yus, *Chem. Rec.*, 2015, **15**, 907–924.
57 R. H. Morris, *Chem. Soc. Rev.*, 2009, **38**, 2282–2291.
58 D. Wang and D. Astruc, *Chem. Rev.*, 2015, **115**, 6621–6686.